

# A Comprehensive Model for Fluidized Bed Coal Combustors

A comprehensive model for the simulation of fluidized bed coal combustors (FBC) is developed, capable of predicting the combustion efficiency, char and limestone elutriation and the corresponding particle size distribution in the bed and in the entrained materials, solids withdrawal rate from the bed, bed temperature profile, sulfur dioxide retention, sulfur dioxide and  $\text{NO}_x$  emissions, concentrations of oxygen, carbon monoxide, carbon dioxide, volatiles, sulfur dioxide and  $\text{NO}_x$  along the combustor height. The model can also simulate combustors with varying cross section along the bed height. The performance of the model is compared with the data obtained from four different combustors. Agreement between the computed results and the data is good. The salient features in the model which need further investigation are pointed out.

RENGA R. RAJAN

and

C. Y. WEN

Department of Chemical Engineering  
West Virginia University  
Morgantown, West Virginia 26506

## SCOPE

A considerable amount of investigation on the performance of fluidized bed combustion system has been under way, particularly in the United States and United Kingdom. Most of the experimental tests have concentrated on feasibility evaluation of FBC. As a result of these studies, pilot plant data related to FBC performance have become available in recent years.

A systematic, theoretical examination of these data has been initiated only recently, and attempts are presently being made to develop theoretical models for predicting the performance of FBC under various operating conditions. Most of the modeling work performed to date has concentrated on a few specific aspects of the fluid bed combustion process. It is the aim of the present work to formulate a comprehensive FBC model taking into account the following elements which were either partially considered or not considered at all in the earlier work.

1. Devolatilization of coal and the subsequent combustion of volatiles and residual char.

2. Sulfur dioxide capture by limestone.
3.  $\text{NO}_x$  release and reduction of  $\text{NO}_x$  by char.
4. Attrition and elutriation of char and limestone.
5. Bubble hydrodynamics.
6. Solids mixing.
7. Heat transfer between gas and solid and solids and heat exchange surfaces.
8. Freeboard reactions.

The uniqueness of the proposed model is its capability to account for the freeboard reactions which may be substantial, the solids mixing within the bed, the devolatilization of coal, sulfur dioxide and  $\text{NO}_x$  release during the combustion of char and volatiles, and the simultaneous absorption of sulfur dioxide by limestone and reduction of  $\text{NO}_x$  by char, the entrainment of char and limestone from the bed and the bubble hydrodynamics in the presence of internal coils.

## CONCLUSIONS AND SIGNIFICANCE

The agreement between the simulated results and the experimental data proves the validity of the proposed model for the fluidized bed coal combustion and of the assumptions made.

Although a simple approach is taken to calculate the bubble size through heat transfer tubes, a proper bubble size correlation in the presence of cooling tubes with different configurations needs to be developed. Bubble size cannot be assumed as an adjustable parameter, and bubble coalescence has to be considered.

The model confirms the importance of the role of solids mixing in maintaining a uniform bed temperature. Poor solids mixing results in nonuniform temperature profile and carbon concentration profile in the bed. The solids mixing is accounted for by the solids mixing parameter in the model. This important parameter in the model also accounts for the devolatilization of coal. The assumption of a major portion of the volatiles being released near the feed point is justified by the concentrations of nitric oxide, oxygen and carbon monoxide observed experimentally near the coal feed point.

Attention has to be focused on the evaluation of the solids

mixing parameter, the fraction of wake solids thrown into the freeboard and the bed to tube heat transfer coefficients. A parametric study indicates the necessity of accurate estimation of these variables for proper accounting of solids mixing, freeboard reactions and bed temperature profile.

Nitric oxide emission is shown to be dependent on the operating temperature. It can be maintained below the EPA limits by maintaining a higher concentration of carbon in the bed and in the freeboard. Nitric oxide concentrations in the bed indicate that most of the nitric oxide is formed in the vicinity of the coal feed point.

In the operation of a FBC, a balance has to be made between the combustion efficiency, the carbon loss, higher sulfur dioxide retention and lower nitric oxide emission.

The present work will aid in the understanding of the performance of FBC under a range of operating conditions. For example, sulfur dioxide, nitric oxide and particulates emissions from the FBC can be estimated for a range of operating conditions. The optimum operating temperature and gas residence time in the bed, which would give maximum combustion efficiency and lower sulfur dioxide and  $\text{NO}_x$  emissions, can be estimated. The temperature profile simulated based on the model will help identify the proper location of cooling coils in the bed to avoid steep temperature gradients for design of coils configuration and packing density.

R. R. Rajan is currently with Exxon Production Research Company, P.O. Box 2189, Houston, TX 77001.

0001-1541-80-2347-0642-\$01.35. ©The American Institute of Chemical Engineers, 1980.

Among the various ways of direct burning of coal, fluidized bed combustion appears to be the most attractive, both from an economic and an environmental standpoint. By carrying out combustion in a fluidized bed combustor (FBC) operating at relatively low temperature (750° to 950°C; 1,382° to 1,742°F), both sulfur dioxide and NO<sub>x</sub> emissions can be maintained at environmentally acceptable levels. In addition, the FBC is well suited for burning low grade, high sulfur coal.

Fluidized bed combustion involves the burning of coal particles in a bed containing limestone/dolomite additives and coal ash. Under normal operating conditions, the coal particles constitute less than 4% of the total solids in the bed. The limestone/dolomite is added to absorb the sulfur dioxide released from coal during combustion. Sulfur dioxide reacts with calcined limestone/dolomite to form calcium sulfate. NO<sub>x</sub> emission is kept low owing to low combustion temperature and by the NO<sub>x</sub> reduction reaction with carbon present in the fluidized bed. The low temperature operation of the fluidized bed offers little, if any, clinker formation of the ash. The heat of combustion is removed by steam coils immersed in the bed. The steam coils also control the temperature of the bed with minimum hindrance to the solids mixing and circulation in the bed. The high heat transfer coefficients between the bed material and the heat exchange surfaces [250 to 420 W/m<sup>2</sup>°K, (45 to 75 Btu/hr ft<sup>2</sup>°F)] and the large heat generation rates [2.0 to 5.0 MW/m<sup>3</sup> (0.193 to 0.483 × 10<sup>6</sup> Btu/hr ft<sup>3</sup>)] in FBC result in a smaller boiler volume for a given duty than the conventional pulverized coal burning boilers.

Attempts have been made to develop mathematical models for predicting the performance of FBC under various operating conditions. (Avedesian and Davidson, 1973; Becker et al., 1975; Baron et al., 1977; Beer, 1977; Borghi et al., 1977; Campbell and Davidson, 1975; Chen and Saxena, 1977; Gibbs et al., 1975; Gibbs, 1975; Gordon and Amundson, 1976; Horio and Wen, 1975, 1978; Horio et al., 1977; Rajan et al., 1978; Park et al., 1979; Sarofim and Beer, 1979). Almost all of these models are based on the two-phase theory of fluidization and address to specific phases of FBC operation. The complexity of the FBC process has been a major hurdle in the development of a comprehensive FBC model. In the present study, an attempt is made to develop such a model that can be employed to simulate the performance of FBC under a wide range of operating conditions.

## MODEL ASSUMPTIONS

The model developed in this study takes into account the following processes occurring in the FBC:

1. Devolatilization of coal, subsequent combustion of volatiles followed by residual char.
2. Sulfur dioxide capture by limestone particles.
3. NO<sub>x</sub> release and reduction of NO<sub>x</sub> by the char.
4. Attrition and elutriation of char and limestone.
5. Bubble hydrodynamics.
6. Solids mixing.
7. Heat transfer between gas and solids and heat exchanger surfaces and bed material.
8. Freeboard reactions.

The following assumptions are made in constructing the FBC model:

1. Single-phase backflow cell model is used for solids mixing calculation.
2. Two-phase bubble assemblage model is adopted for gas phase material balances.
3. Solids exchange between the bubble phase and emulsion phase is assumed to be rapid.
4. Bubble size is a function of bed diameter and height above the distributor. When cooling tubes are present, bubble size in the tubes region of the bed is based on the horizontal pitch distance between the tubes.
5. Bubbles and clouds are both combined into the bubble phase. The gas interchange coefficient between the bubble and

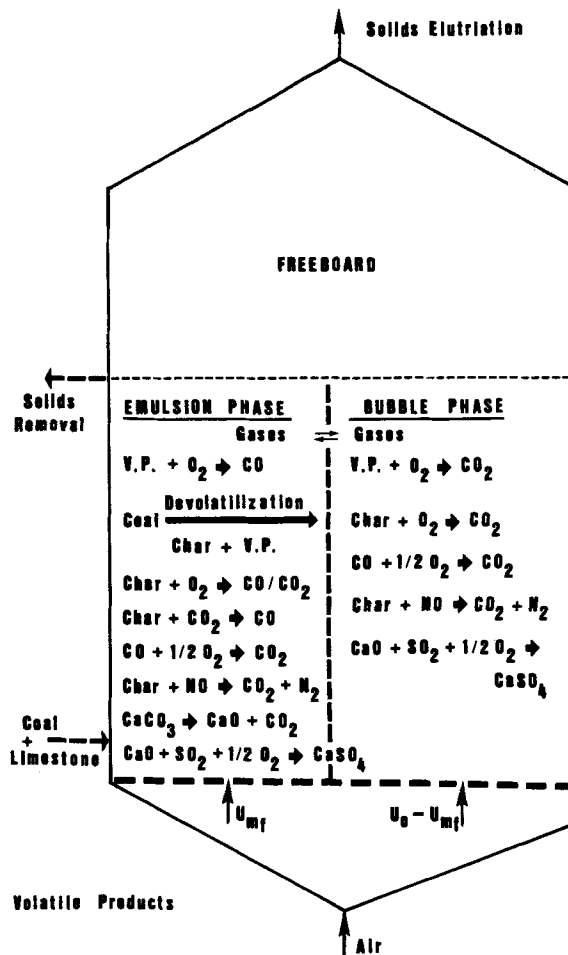


Figure 1. Schematic illustration of the FBC.

emulsion phases is a function of the bubble size and is distributed axially.

6. The gas flow rate through the emulsion phase corresponds to minimum fluidization velocity.

7. Devolatilization of coal is neither instantaneous nor uniform in the bed. It is assumed that volatiles release rate is proportional to the solids mixing rate.

8. Volatiles are assumed to be released in the emulsion phase.

9. Volatile nitrogen and sulfur increase as a function of bed temperature (Fine et al., 1974).

10. Sulfur and nitrogen in the residual char are assumed to be released as sulfur dioxide and NO<sub>x</sub> during the combustion of char.

## MODEL BACKGROUND

The various physicochemical processes occurring in the FBC are shown in Figure 1. The basic elements of the overall combustion process are discussed below.

### Devolatilization and Combustion of Char

Coal particles fed to the hot combustor are rapidly heated while undergoing devolatilization (or pyrolysis). The volatile matter of coal is evolved into the particulate phase or emulsion phase of the bed. The bed temperature and the proximate volatile matter content of coal determine the yield of volatiles. Volatile yield is estimated by the following empirical correlations (Gregory and Littlejohn, 1965):

$$V = VM - A - B$$

$$A = \exp(26.41 - 3.961 \ln t + 0.0115 VM)$$

$$B = 0.2(VM - 10.9)$$

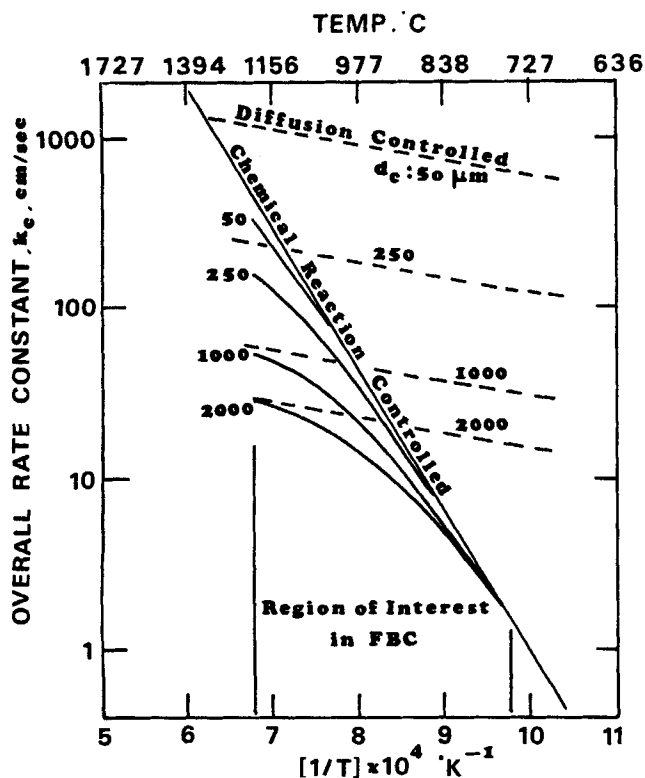


Figure 2. Rate controlling regimes in FBC.

The composition of the products of devolatilization in weight fractions is estimated from the following correlations developed from the experimental data of Loison and Chauvin (1964):

$$\begin{aligned} \text{CH}_4 &= 0.201 - 0.469 X_{VM} + 0.241 X_{VM}^2 \\ \text{H}_2 &= 0.157 - 0.868 X_{VM} + 1.388 X_{VM}^2 \\ \text{CO}_2 &= 0.135 - 0.900 X_{VM} + 1.906 X_{VM}^2 \\ \text{CO} &= 0.428 - 2.653 X_{VM} + 4.845 X_{VM}^2 \\ \text{H}_2\text{O} &= 0.409 - 2.389 X_{VM} - 4.554 X_{VM}^2 \\ \text{Tar} &= -0.325 + 7.279 X_{VM} - 12.880 X_{VM}^2 \end{aligned}$$

Volatile nitrogen released during devolatilization is expressed as (Fine et al., 1974)

$$V_N = 0.001 T - 0.6 \text{ g/g coal (d.b.)}$$

and volatile sulfur is expressed as

$$V_S = 0.001 T - 0.06 \text{ g/g coal (d.b.)}$$

Despite extensive research on coal devolatilization, reliable rate expressions for coal devolatilization are not available to date. Particularly, the rate of devolatilization in relation to the rate of solids mixing in a fluidized bed is not well known. The time required for the process of devolatilization to complete depends on the coal particle size and the temperature of the fluidized bed. Beer (1977) estimated that 0.5 to 1 s is required for a 1 mm coal particle to complete the devolatilization in a FBC. Wen and Chen (1979) estimated that 3 s at 900°C and 4 s. at 800°C are required for the devolatilization of subbituminous coal in a limestone bed. On the other hand, the time required for the solids to mix in a FBC depends on the size of the bed and number of feed points located in the bed. Solid mixing time for a 0.61 m<sup>2</sup> combustor with a bed height of 1.22 m and a superficial gas velocity of 1.22 m/s lies in the range of 2 to 10 s, depending on whether internals are present or not. Hence it is more likely that a major portion of the volatiles will be released near the coal feed point. In this model, the volatiles are assumed to be released in two ways. A portion of volatiles proportional to  $f_w$ , the solids mixing coefficient (also the fraction of bubble volume occupied by the wake), is released uniformly throughout the bed. The remaining portion of volatiles proportional to  $(1 - f_w)$  is released near the coal feed point.

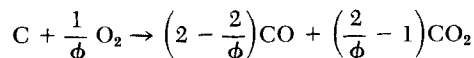
At temperatures above 650°C and in an oxidizing atmosphere, the rate of burning of volatiles is fast compared to the time

required for volatiles evolution. However, the combustion of volatiles released in the emulsion phase is controlled by the availability of oxygen in the emulsion phase. Since the oxygen concentration in the emulsion phase is low, the volatile gases in the emulsion phase first tend to form carbon monoxide by partial combustion, whereas the volatiles exchanged to the bubble phase burn completely to carbon dioxide because of excess oxygen present in the bubble phase.

The rate of burning of carbon monoxide is expressed as (Hotte et al., 1965)

$$\text{CO} + \frac{1}{2} \text{O}_2 \rightarrow \text{CO}_2, r_{\text{CO}} = 3 \times 10^{10} \left( \frac{P}{R_g T} \right)^{1.8} \exp(-6.699 \times 10^7 / RT) Y_{\text{H}_2\text{O}}^{0.5} \cdot Y_{\text{CO}} \frac{17.5 Y_{\text{O}}}{1 + 24.7 Y_{\text{O}}} \text{ gmole/cm}^3 \text{ s}$$

Residual char burns according to the reaction



where  $\phi$  is a mechanism factor which takes the value 1 when carbon dioxide is transported away from the char particle and 2 when carbon monoxide is transported away during char combustion (Field et al., 1967). The factor  $\phi$  is a function of char particle diameter and temperature. For small particles, carbon monoxide formed during char combustion diffuses out fast because of rapid mass transfer and burns to form carbon dioxide outside the particle, whereas for large particles, because of slower mass transfer, carbon monoxide burns within the boundary layer of the particle, and carbon dioxide is transported out.  $\phi$  is expressed as

$$\begin{aligned} \phi &= \frac{2p + 2}{p + 2} \quad \text{for } d_c < 0.005 \text{ cm} \\ \phi &= \frac{(2p + 2) - p(d_c - 0.005)/0.095}{p + 2} \quad \text{for } 0.005 < d_c < 0.1 \text{ cm} \end{aligned}$$

where  $p$  is the ratio of carbon monoxide to carbon dioxide formed during char combustion and is given by (Arthur, 1951)

$$p = 2,500 \exp(-5.19 \times 10^7 / RT)$$

The rate expression for char combustion is estimated by Field et al. (1967)

$$r_c^* = \pi d_c^2 k_c C_{\text{O}_2} \text{ gmole/s particle}$$

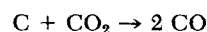
where  $k_c$  is the overall rate constant and is given by

$$k_c = \frac{R_g T_m / M_c}{\frac{1}{k_{cR}} + \frac{1}{k_{cf}}} \text{ cm/s}$$

$$\begin{aligned} k_{cR} &= \text{chemical reaction rate constant} \\ &= 8,710 \exp(-1.4947 \times 10^8 / RT_c) \text{ g/cm}^2 \cdot \text{s} \cdot \text{atm} \end{aligned}$$

$$\begin{aligned} k_{cf} &= \text{diffusion rate constant} \\ &= 24 \phi D / d_c R_g T_m \text{ g/cm}^2 \cdot \text{s} \cdot \text{atm} \end{aligned}$$

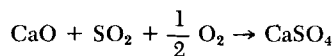
For smaller particles, diffusion of oxygen to the surface of the char particle is faster than the chemical reaction rate of combustion, while for larger particles, diffusion of oxygen is slower than the chemical rate. Thus, the diffusional term tends to dominate for larger particles at high temperatures, while the chemical term tends to dominate at low temperatures (Figure 2). Carbon dioxide formed during combustion reacts with char according to



and the rate expression for the above reaction is  $r_{\text{CO}_2} = \pi d_c^2 k_{\text{CO}_2} C_{\text{CO}_2} \text{ gmole/s} \cdot \text{particle}$ , where  $k_{\text{CO}_2} = 4.1 \times 10^8 \exp(-2.478 \times 10^8 / RT) \text{ cm/s}$  (Caram and Amundson, 1977).

## Sulfur Dioxide—Limestone Reaction

When limestone is added to a fluidized bed burning coal, the sulfur dioxide released from the combustion of coal reacts with calcined limestone according to



The reaction rate of a limestone particle can be expressed as (Borgwardt, 1970; Wen and Ishida, 1973)

$$r_l = \frac{\pi}{6} d_l^3 k_{rl} C_{\text{SO}_2} \quad \text{gmole/s particle}$$

where  $k_{rl}$  is the overall volumetric reaction rate constant and is a rapidly decreasing function of limestone conversion  $f_l$ . The overall reaction rate constant  $k_{rl}$  is calculated by

$$k_{rl} = k'_{rl} S_g \lambda_l$$

where  $k'_{rl}$  is equal to  $490 \exp(-7.33 \times 10^7/RT)$  g/cm<sup>3</sup>s. The value of activation energy was obtained by Wen and Ishida (1973). By using Borgwardt's data (1971), the specific surface area  $S_g$  is correlated with calcination temperature as

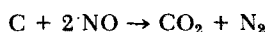
$$S_g = -38.4 T + 5.6 \times 10^4, \text{ cm}^2/\text{g for } T \geq 1,253^\circ\text{K}$$

$$= 35.9 T - 3.67 \times 10^4, \text{ cm}^2/\text{g for } T < 1,253^\circ\text{K}$$

$\lambda_l$ , the reactivity of limestone, is a function of conversion, temperature and particle size. Calcium sulfate formed owing to the sulfation of calcined limestone tends to block the pores formed during limestone calcination, building an impervious layer on the particle surface and reducing the reactivity of limestone. The reactivity of limestone is calculated using the grain model developed by Ishida and Wen (1973) and is presented in Rajan et al. (1978).

## NO<sub>x</sub>-Char Reaction

Nitrogen oxides are generated during the combustion of volatiles and char and are subsequently reduced to nitrogen by reaction with nitrogeneous fragments (containing ammonia) in the volatiles and also by the heterogeneous reaction with char. Fuel nitrogen compounds in the volatiles would be in the form of ammonia. When the volatiles burn, ammonia is oxidized to nitric oxide. When the residual char burns, nitrogeneous fragments of the char are also oxidized to nitric oxide. The released nitrogen oxides are reduced by char according to the reaction



The rate expression for nitric oxide reduction is

$$r_{\text{NO}} = \pi d_c^2 k_{\text{NO}} C_{\text{NO}} \quad \text{gmole NO/s} \cdot \text{particle}$$

where  $k_{\text{NO}} = 5.24 \times 10^7 \exp(-1.424 \times 10^8/RT_m)$  cm/s (Oguma et al., 1977; Horio et al., 1977).

## Attrition and Entrainment of Char and Limestone

Limestone and char particles in the bed are subjected to erosion and attrition owing to the rapid mixing of the solids. The attrition rate is proportional to the rate of energy input. The size distribution of the fines produced has been found to be approximately constant for a particular bed material and independent of the bed size distribution or operating conditions (Merrick and Highley, 1974). The rate of energy input to the bed particles is taken to be proportional to  $(U_0 - U_{mf})$  and also to the bed weight. The rate of production of fines is correlated as

$$R_a = K(U_0 - U_{mf})M_b \quad \text{g/s}$$

The value of  $K$  is dependent on the friability of the material. The values of  $K$  lie in the range  $9.11 \times 10^{-8}$  for ash and  $2.73 \times 10^{-8}$  for limestone.

The rate of elutriation of char and limestone for a size fraction  $x$  is directly proportional to their concentration in the bed; that is

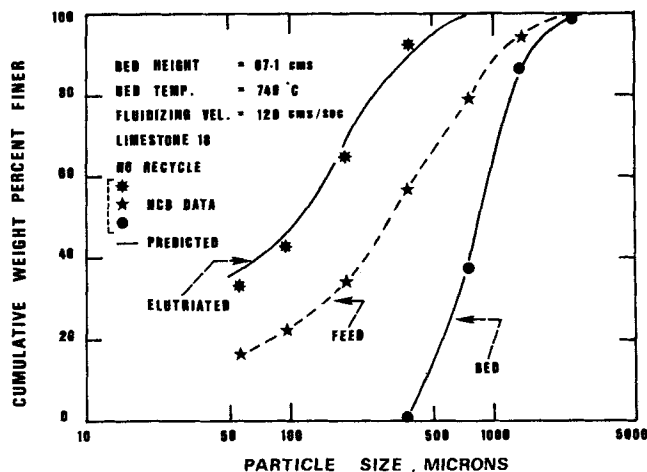


Figure 3. Size distributions of the particles in the FBC.

$$R_x = E_x b_x \quad \text{g/s}$$

There are many correlations proposed to calculate the elutriation rate constant  $E_x$ . Many of the correlations exhibit an improper qualitative behavior in the smaller particle size ranges. A recent correlation proposed by Merrick and Highley (1974) accounts properly for the boundary conditions of a maximum limiting elutriation rate constant at zero particle size and the rate constant approaching zero with increasing particle size and at  $U_0 = U_{mf}$ . It is of the form

$$E_x = G \exp \left[ -10.4 \left( \frac{U_t}{U_0} \right)^{0.5} \left( \frac{U_{mf}}{U_0 - U_{mf}} \right)^{0.25} \right] \quad \text{g/s}$$

The above correlation was obtained by Merrick and Highley with data from NCB combustor in which the freeboard height was around 275 cm. When this correlation is used to simulate the performance of NCB combustor, the results agree well with data (Figure 3). This correlation does not take into account the entrainment below the transport disengage height, or TDH, which is defined as the critical freeboard height above which the rate of entrainment of fines remains constant. In view of the fact that the entrainment below TDH is dependent on the freeboard height, the following correlation is suggested to calculate the entrainment rate as a function of height above the bed surface. The rate of entrainment is given by

$$R_x = F_{0,x} \exp \left[ \frac{h}{275.0} \cdot \ln \left( \frac{E_x b_x}{F_{0,x}} \right) \right] \quad \text{g/s} \quad (1)$$

where the constant 275.0 represents the freeboard height of the NCB combustor.

When the bubbles burst at the surface of the bed, solids in the wake of the bubbles are thrown into the freeboard. The amount of solids splashed into the freeboard can be calculated from (Yates and Rowe, 1977)

$$F_0 = A_t \cdot (U_0 - U_{mf}) f_{uc} (1 - \epsilon_{mf}) \rho_s \cdot f_{sw} \quad \text{g/s} \quad (2)$$

There are many correlations available in the literature to calculate the TDH (Zenz and Weil, 1958; Amitin et al., 1968; Nazemi et al., 1973; Fournol et al., 1973). The correlation proposed by Amitin et al. (1968) is used here because of its simplicity and accuracy in the range of fluidizing velocities encountered in the combustor:

$$\text{TDH} = 0.147 \bar{U}_0^{1.2} (22.4 - 1.2 \ln \bar{U}_0) \quad \text{cm}$$

TDH is compared with the actual height (height between the bed surface and the flue gas exit). If the TDH is smaller than the actual freeboard height, then TDH is used to calculate the solids elutriation rate. Entrainment rate of solids as a function of the height above the bed surface is calculated using Equation (1).

## Freeboard Reactions

Char combustion, sulfur dioxide absorption and  $\text{NO}_x$  reduction reactions take place in the freeboard. Heat generated by combustion and heat carried by the flue gases are removed by the cooling coils present in the freeboard. The hydrodynamics in the freeboard is different from that in the bed. There are no bubbles present in the freeboard. Any unburnt volatiles from the bed would be burnt in the freeboard.

The freeboard region is divided into a number of compartments of equal size. The compartment size in the freeboard region is estimated based on the Peclet number in the freeboard region using the following correlations (Wen and Fan, 1975):

$$N_{Re} = D_t \bar{U}_0 \rho_g / \mu$$

$$N_{Pe} = \bar{U}_0 D_t / E_z$$

$$N_{Sc} = \mu / D \rho_g$$

$$\frac{1}{N_{Pe}} = \frac{1}{N_{Re} N_{Sc}} + \frac{N_{Re} N_{Sc}}{192} \quad \text{for } N_{Re} < 2,000$$

$$\frac{1}{N_{Pe}} = \frac{3 \times 10^7}{N_{Re}^{2.1}} + \frac{1.35}{N_{Re}^{1.8}} \quad \text{for } N_{Re} > 2,000$$

If we know the axial dispersion coefficient  $E_z$ , the average compartment size in the freeboard is calculated as

$$\Delta Z = \frac{2 E_z}{\bar{U}_0}$$

The concentrations of gaseous species vary with each compartment, although the concentrations are uniform (completely mixed) within each compartment. If we know the average height of each compartment above the bed surface, the solids entrainment rate at that height is calculated. Residence time of solids in each compartment is given by  $\Delta Z / (U_0 - U_T)$ , where  $\Delta Z$  is the compartment size. Solids holdup in each compartment is then obtained from

$$\text{Solids holdup in each compartment} = \frac{(\text{upward} + \text{downward}) \text{ flow rate of solids}}{\text{solids} \times \text{residence time of solids in that compartment}}$$

Depending on the residence time of particles in the freeboard, and the char particles burning time, char particles will either be partially or completely burnt, and the unburnt char particles are elutriated. The burning time of a char particle is estimated from (Field et al., 1967)

$$t_b = \text{burning time of a char particle} \\ = \rho_{c, ch} R_g T_m d_c^2 / (96 \phi D P_{O_2})$$

Background information on sulfur dioxide-limestone reaction, bubble hydrodynamics, solids mixing and heat transfer are discussed elsewhere (Horio and Wen, 1978; and Rajan et al., 1978).

## MODEL DESCRIPTION

### Elutriation Calculations

A mathematical model has been developed for elutriation in a fluid bed system with size reduction and recycle to the bed of some or all of the fines from the primary and/or secondary cyclones. The model takes into account the variation in the rates of elutriation and size reduction with particle size. If the size reduction is due to more than one process, then there will be separate values of size reduction constant for each process. In general, the rates of size reduction by the separate processes in each size fraction are additive. A mass balance is performed for each size fraction  $x$  as follows (Merrick and Highley, 1974):

$$\begin{array}{l} W_{f,x} + W_{x-1} + a_x k_x M_x \\ \text{(feed rate)} \quad \text{(gain of particles} \quad \text{(gain of fines} \\ \quad \quad \quad \text{from next largest} \quad \text{produced by abrasion)} \end{array}$$

size due to size  
reduction)

$$= M_x W_D / M_b + R_x q_{1x} (1 - p_1) + R_x q_{2x} (1 - q_{1x}) (1 - P_2) \\ \text{(withdrawal} \quad \text{(particles cap-} \quad \text{(particles captured} \\ \text{rate from the} \quad \text{tured by pri-} \quad \text{by secondary cyclone} \\ \text{bed)} \quad \text{mary cyclone} \quad \text{but not recycled)}$$

$$+ R_x (1 - q_{1x}) (1 - q_{2x}) + k_x M_x \\ \text{(particulate emission)} \quad \text{(loss of weight due to} \\ \quad \quad \quad \text{production of fines by} \\ \quad \quad \quad \text{abrasion)}$$

$$+ W_x \\ \text{(loss of particles to next smallest} \\ \text{size due to size reduction)}$$

The rate of loss of particles to the next smallest size  $W_x$  is determined by considering a mass of particles  $M_x$  at size  $d_x$  and by calculating the mass remaining  $M_{x+1}$  after the size has been reduced to  $d_{x+1}$ . The rate of reduction is written as

$$\frac{dM}{d\theta} = -k_x M (U_0 - U_{mf}) \quad (3)$$

The rate of size reduction between  $d_x$  and  $d_{x+1}$  is

$$\frac{dd_x}{d\theta} = \frac{-k_x}{3} d_x (U_0 - U_{mf}) \quad (4)$$

Dividing Equation (3) by Equation (4), we get

$$\frac{dM}{dd_x} = \frac{3M}{d_x}$$

and integrating between  $d_x$  and  $d_{x+1}$  we get

$$\frac{M_{x+1}}{M_x} = \left( \frac{d_{x+1}}{d_x} \right)^3$$

This fraction is the proportion of the total feed to the  $x^{\text{th}}$  size fraction which is reduced in diameter to  $(x+1)^{\text{th}}$  size fraction. Therefore,  $W_x = [W_{f,x} + a_x K(U_0 - U_{mf}) M_b + W_{x-1}] (d_{x+1}/d_x)^3$ . For the coarsest size fraction,  $W_{x-1}$  is zero.

The entire calculation is iterative, starting from initial guesses of the withdrawal rate of solids from the bed and the size distribution of particles in the bed. Mass balance is performed on each successive close size fraction, starting from the coarsest. The bed weight in each size fraction and hence the total bed weight and bed size distribution of limestone are calculated. The procedure is repeated till the calculated total bed weight based on each size fraction equals the bed weight computed from bed height and density. The elutriation rate, fines collection/recycle rates, particle emission and size distribution of elutriated particles are then calculated.

### Material and Energy Balances

Material balances are made for volatile gases, carbon monoxide, carbon dioxide, oxygen, sulfur dioxide and nitric oxide in the bubble and emulsion phases within the bed and in the freeboard. Material balance of water is not included because carbon-steam reaction is slow and has been ignored. Depending on the concentration of oxygen in the emulsion phase, different material balances are used as shown below.

**Case A:** Volatile concentration in the emulsion phase is not zero because of insufficient oxygen in emulsion phase for complete combustion of volatiles. Char and carbon monoxide combustion do not proceed in the emulsion phase.

### EMULSION PHASE EQUATIONS

Oxygen:

$$Y_{E,i} = 0.0 \quad (5)$$

Volatiles:

$$\begin{aligned}
F_{EM,i} Y_{E,v,i} &= F_{EM,i-1} Y_{E,v,i-1} - a_1 Y_{E,v,i-1} && \text{by char} && \text{by CO} && \text{by volatiles} \\
(\text{volatiles out}) &(\text{volatiles in}) && \text{combustion)} && \text{combustion)} && \text{burning)} \\
&&& (\text{volatiles exchanged} && && \\
&&& \text{to bubble phase}) && && \\
&&& - \frac{(F_{EM,i-1} Y_{E,i-1} + a_1 Y_{B,i})}{X_{O_2}} + R_{v,i} && && \\
&&& (\text{volatiles burnt}) && (\text{volatiles released} && \\
&&& && \text{during devolatilization}) && 
\end{aligned} \quad (6)$$

where  $a_1 = K_{BE,i} A_{t,i} \Delta Z_i \epsilon_{B,i} P/R_g T_i$ , gmole/s

Carbon monoxide:

$$\begin{aligned}
F_{EM,i} Y_{E,CO,i} &= F_{EM,i-1} Y_{E,CO,i-1} - a_1 Y_{E,CO,i} && (\text{CO out}) && (\text{CO in}) && (\text{CO exchanged to} \\
&&& && && \text{bubble phase}) \\
&&& - \frac{(F_{EM,i-1} Y_{E,i-1} + a_1 Y_{B,i})}{X_{O_2}} + V_{CO} + R_{CO,i} && && \\
&&& (\text{CO produced by volatiles} && (\text{CO released during} && \\
&&& \text{burning}) && \text{devolatilization}) && \\
&&& + \frac{2 a_4 Y_{E,CO_2,i}}{(\text{CO produced by C—CO}_2 \text{ reaction})} && && 
\end{aligned} \quad (7)$$

where

$$a_4 = a_m A_{t,i} \Delta Z_i (1 - \epsilon_{c,i} - \epsilon_{tube,i}) (k_{CO_2,i} \frac{P}{R_g T_{E,i}} X_i), \text{ gmole/s}$$

$$a_m = \frac{6 \rho_b (1 - \epsilon_{mf})}{d_c \rho_{ch} C_{ch}}$$

Carbon dioxide:

$$\begin{aligned}
F_{EM,i} Y_{E,CO_2,i} &= F_{EM,i-1} Y_{E,CO_2,i-1} - a_1 (Y_{E,CO_2,i} - Y_{B,CO_2,i}) && (\text{CO}_2 \text{ out}) && (\text{CO}_2 \text{ in}) && (\text{CO}_2 \text{ exchanged to} \\
&&& && && \text{bubble phase}) \\
&&& + \frac{R_{CO_2,i}}{(\text{CO}_2 \text{ released during} && - \frac{a_4 Y_{E,CO_2,i}}{(\text{CO}_2 \text{ consumed by} && \\
&&& \text{devolatilization})} && \text{C—CO}_2 \text{ reaction})} && 
\end{aligned} \quad (8)$$

## BUBBLE PHASE EQUATIONS

Oxygen:

$$\begin{aligned}
F_{BM,i} Y_{B,i} &= F_{BM,i-1} Y_{B,i-1} - a_1 Y_{B,i} && (\text{oxygen out}) && (\text{oxygen in}) && (\text{oxygen exchanged to} \\
&&& && && \text{emulsion phase}) \\
&&& - a_2 Y_{B,i} - \frac{a_1 Y_{E,CO,i}}{2} && && \\
&&& (\text{oxygen consumed} && (\text{oxygen consumed by} && \\
&&& \text{by char}) && \text{CO exchanged to} && \\
&&& && \text{bubble phase}) && \\
&&& - a_1 Y_{E,v,i} X_{O_2,c} && && \\
&&& (\text{oxygen consumed by} && (\text{oxygen consumed by} && \\
&&& \text{volatiles exchanged} && \text{volatiles exchanged} && \\
&&& \text{to bubble phase}) && \text{to bubble phase}) && 
\end{aligned} \quad (9)$$

where

$$a_2 = a_m A_{t,i} \Delta Z_i (\epsilon_{c,i} - \epsilon_{B,i}) k_{CB,i} \frac{P}{R_g T_{B,i}} X_i$$

Carbon dioxide:

$$\begin{aligned}
F_{BM,i} Y_{B,CO_2,i} &= F_{BM,i-1} Y_{B,CO_2,i-1} - a_1 (Y_{B,CO_2,i} - Y_{E,CO_2,i}) && (\text{CO}_2 \text{ out}) && (\text{CO}_2 \text{ in}) && (\text{CO}_2 \text{ exchanged to} \\
&&& && && \text{emulsion phase}) \\
&&& + a_2 Y_{B,i} + a_1 Y_{E,CO,i} + a_1 Y_{E,v,i} V_{CO_2} && && \\
&&& (\text{CO}_2 \text{ produced} && (\text{CO}_2 \text{ produced} && (\text{CO}_2 \text{ produced} && \\
&&& && && && 
\end{aligned}$$

## FREEBOARD EQUATIONS

Oxygen:

$$Y_{O,i} = 0.0 \quad (10)$$

Volatiles:

$$F_{MT} Y_{v,i} = F_{MT} Y_{v,i-1} - F_{MT} Y_{O,i-1}/X_{O_2} \quad (11)$$

Carbon monoxide:

$$\begin{aligned}
F_{MT} Y_{CO,i} &= F_{MT} Y_{CO,i-1} + \frac{2 a'_4 Y_{CO_2,i}}{(\text{CO out})} && (\text{CO in}) && (\text{CO produced by} \\
&&& && \text{C—CO}_2 \text{ reaction}) && \\
&&& + \frac{F_{MT} (Y_{v,i-1} - Y_{v,i}) V_{CO}}{(\text{CO produced by volatiles burning})} && && 
\end{aligned} \quad (12)$$

where

$$a'_4 = \frac{P}{R_g T_{B,i}} N_{c,i} \pi d_{ce,i}^2 k_{CO_2,i}, \text{ gmole/s}$$

Carbon dioxide:

$$F_{MT} Y_{CO_2,i} = F_{MT} Y_{CO_2,i-1} - a'_4 Y_{CO_2,i} \quad (13)$$

Case B: Sufficient oxygen is present in the emulsion phase for the combustion of volatiles.

## EMULSION PHASE EQUATIONS

Volatiles:

$$Y_{E,v,i} = 0.0 \quad (14)$$

Oxygen:

$$\begin{aligned}
F_{EM,i} Y_{E,i} &= F_{EM,i-1} Y_{E,i-1} - a_1 (Y_{E,i} - Y_{B,i}) && (\text{oxygen out}) && (\text{oxygen in}) && (\text{oxygen exchanged to} \\
&&& && && \text{bubble phase}) \\
&&& - a_3 Y_{E,i}/\phi_{E,i} - (F_{EM,i-1} Y_{E,v,i-1} + R_{v,i}) X_{O_2} && && \\
&&& (\text{oxygen consumed} && (\text{oxygen consumed by volatiles} && \\
&&& \text{by char}) && \text{burning}) && \\
&&& - k Y_{E,CO,i} \left( \frac{17.5 Y_{E,i}}{1 + 24 \cdot 7 Y_{E,i}} \right) / 2.0 && && \\
&&& (\text{oxygen consumed by CO}) && && 
\end{aligned} \quad (15)$$

where

$$\begin{aligned}
k &= 3 \times 10^{10} \exp(-6.699 \times 10^7/RT_i) \left( \frac{P}{R_g T_i} \right)^{1.8} Y_{H_2O}^{0.5} \\
&\quad \times A_{t,i} \Delta Z_i (1 - \epsilon_{c,i} - \epsilon_{tube,i}) \epsilon_{mf} \text{ gmole/s} \\
a_3 &= a_m A_{t,i} \Delta Z_i (1 - \epsilon_{c,i} - \epsilon_{tube,i}) k_{CE,i} \frac{P}{R_g T_{E,i}} X_i
\end{aligned}$$

Carbon monoxide:

$$\begin{aligned}
F_{EM,i} Y_{E,CO,i} &= F_{EM,i-1} Y_{E,CO,i-1} && (\text{CO out}) && (\text{CO in}) && \\
&&& - k Y_{E,CO,i} \left( \frac{17.5 Y_{E,i}}{1 + 24 \cdot 7 Y_{E,i}} \right) && && \\
&&& (\text{CO burnt}) && && \\
&&& + \frac{(F_{EM,i-1} Y_{v,i-1} + R_{v,i}) V_{CO}}{(\text{CO produced by volatiles} && + \frac{R_{CO,i}}{(\text{CO released during} && \\
&&& \text{burning})} && \text{devolatilization})} && \\
&&& + 2 a_4 Y_{E,CO_2,i} + a_3 \left( 2 - \frac{2}{\phi_{E,i}} \right) Y_{E,i} && && 
\end{aligned} \quad (16)$$

(CO produced by  
C—CO<sub>2</sub> reaction)

(CO produced by  
char combustion)

$$- k' Y_{CO,i} \left( \frac{17.5 Y_{O,i}}{1.24 \cdot 7 Y_{O,i}} \right) \quad (23)$$

(CO burnt)

Carbon dioxide:

$$\begin{aligned} F_{EM,i} Y_{E,CO_2,i} &= F_{EM,i-1} Y_{E,CO_2,i-1} - a_1(Y_{E,CO_2,i} - Y_{B,CO_2,i}) \\ &\quad \text{(CO}_2 \text{ out)} \quad \text{(CO}_2 \text{ in)} \quad \text{(CO}_2 \text{ exchanged to bubble phase)} \\ &+ k Y_{E,CO,i} \left( \frac{17.5 Y_{E,i}}{1 + 24 \cdot 7 Y_{E,i}} \right) + R_{CO_2,i} \\ &\quad \text{(CO}_2 \text{ produced by CO combustion)} \quad \text{(CO}_2 \text{ released during devolatilization)} \\ &- a_4 Y_{E,CO_2,i} + a_3 \left( \frac{2}{\phi_{E,i}} - 1 \right) Y_{E,i} \quad (18) \\ &\quad \text{(CO}_2 \text{ consumed by C—CO}_2 \text{ reaction)} \quad \text{(CO}_2 \text{ produced by char combustion)} \end{aligned}$$

## BUBBLE PHASE EQUATIONS

Oxygen:

$$\begin{aligned} F_{BM,i} Y_{B,i} &= F_{BM,i-1} Y_{B,i-1} - a_1(Y_{B,i} - Y_{E,i}) \\ &\quad \text{(oxygen out)} \quad \text{(oxygen in)} \quad \text{(oxygen exchanged to emulsion phase)} \\ &- a_2 Y_{B,i} - a_1(Y_{E,CO,i}/2 \\ &\quad \text{(oxygen consumed by char)} \quad \text{(oxygen consumed by CO exchanged to bubble phase)} \end{aligned} \quad (19)$$

Carbon dioxide:

$$\begin{aligned} F_{BM,i} Y_{B,CO_2,i} &= F_{BM,i-1} Y_{B,CO_2,i-1} - a_1(Y_{B,CO_2,i} - Y_{E,CO_2,i}) \\ &\quad \text{(CO}_2 \text{ out)} \quad \text{(CO}_2 \text{ in)} \quad \text{(CO}_2 \text{ exchanged to emulsion phase)} \\ &+ a_2 Y_{B,i} + a_1 Y_{E,CO,i} \quad (20) \\ &\quad \text{(CO}_2 \text{ produced by char combustion)} \quad \text{(CO}_2 \text{ produced by CO combustion)} \end{aligned}$$

## FREEBOARD EQUATIONS

Volatiles:

$$Y_{r,i} = 0.0 \quad (21)$$

Oxygen:

$$\begin{aligned} F_{MT} Y_{O,i} &= F_{MT} Y_{O,i-1} - F_{MT} Y_{r,i-1} X_{O_2} \\ &\quad \text{(oxygen out)} \quad \text{(oxygen in)} \quad \text{(oxygen consumed by volatiles)} \\ &- k' Y_{CO,i} \left( \frac{17.5 Y_{O,i}}{1 + 24 \cdot 7 Y_{O,i}} \right) / 2 - a'_2 Y_{O,i} / \phi_{B,i} \quad (22) \\ &\quad \text{(oxygen consumed by CO combustion)} \quad \text{(oxygen consumed by char combustion)} \end{aligned}$$

where

$$\begin{aligned} k' &= 3 \times 10^{10} \exp(-6.699 \times 10^7 / RT_i) \\ &\quad \left( \frac{P}{R_g T_i} \right)^{1.8} Y_{H_2O}^{0.5} A_{t,i} \Delta Z_i (1 - \epsilon_{tube,i}), \text{ gmole/s} \\ a'_2 &= \left( \frac{P}{R_g T_{B,i}} \right) N_{c,i} \pi d_{ce,i}^2 k_{c,i}, \text{ gmole/s} \end{aligned}$$

Carbon monoxide:

$$\begin{aligned} F_{MT} Y_{CO,i} &= F_{MT} Y_{CO,i-1} + 2 a'_4 Y_{CO,i} \\ &\quad \text{(CO out)} \quad \text{(CO in)} \quad \text{(CO produced by C—CO}_2 \text{ reaction)} \\ &+ F_{MT} Y_{r,i-1} V_{CO} + a'_2 Y_{O,i} \left( 2 - \frac{2}{\phi_{B,i}} \right) \\ &\quad \text{(CO produced by volatiles burning)} \quad \text{(CO produced by char combustion)} \end{aligned}$$

Carbon dioxide:

$$\begin{aligned} F_{MT} Y_{CO_2,i} &= F_{MT} Y_{CO_2,i-1} - a'_4 Y_{CO_2,i} \\ &\quad \text{(CO}_2 \text{ out)} \quad \text{(CO}_2 \text{ in)} \quad \text{(CO}_2 \text{ consumed by C—CO}_2 \text{ reaction)} \\ &+ a'_2 Y_{O,i} \left( \frac{2}{\phi_{B,i}} - 1 \right) + k' Y_{CO,i} \left( \frac{17.5 Y_{O,i}}{1 + 24 \cdot 7 Y_{O,i}} \right) \\ &\quad \text{(CO}_2 \text{ produced by char combustion)} \quad \text{(CO}_2 \text{ produced by CO combustion)} \end{aligned} \quad (24)$$

The boundary conditions are

$$\begin{aligned} Y_{B,1} &= 0.21 F_{MF} / F_{MT} \\ Y_{E,1} &= Y_{B,1} \\ Y_{E,r,1} &= 0.0 \\ Y_{E,CO,1} &= 0.0 \\ Y_{E,CO_2,1} &= 0.0 \\ Y_{B,CO_2,1} &= 0.0 \end{aligned}$$

## SULFUR DIOXIDE AND NITRIC OXIDE BALANCES

Nitrogen and sulfur content in the volatile products released during devolatilization is a function of bed temperature. Volatile nitrogen increases from 20 to 70% as temperature rises from 800° to 1,300°K (Fine et al., 1974). Sulfur and nitrogen left in the residual char are released as sulfur dioxide and nitrogen oxide when char burns. The following material balances are made for sulfur dioxide and nitrogen oxide in the bed and in the freeboard.

## EMULSION PHASE EQUATIONS

$$\begin{aligned} F_{EM,i} Y_{E,SO_2,i} &= F_{EM,i-1} Y_{E,SO_2,i-1} - a_1(Y_{E,SO_2,i} - Y_{B,SO_2,i}) \\ &\quad \text{(SO}_2 \text{ out)} \quad \text{(SO}_2 \text{ in)} \quad \text{(SO}_2 \text{ exchanged to bubble phase)} \\ &- a_{E,SO_2,i} Y_{E,SO_2,i} + R_{E,SO_2,c,i} \\ &\quad \text{(SO}_2 \text{ absorbed by limestone)} \quad \text{(SO}_2 \text{ released during char combustion)} \\ &+ R_{E,SO_2,v,i} \quad (25) \\ &\quad \text{(SO}_2 \text{ released during volatiles combustion)} \end{aligned}$$

where

$$\begin{aligned} a_{E,SO_2,i} &= A_{t,i} \Delta Z_i (1 - \epsilon_{c,i} - \epsilon_{tube,i}) \\ &\quad (1 - \epsilon_{mf}) k_{rl} \left( \frac{P}{R_g T_i} \right), \text{ gmole/s} \end{aligned}$$

$$\begin{aligned} F_{EM,i} Y_{E,NO,i} &= F_{EM,i-1} Y_{E,NO,i-1} - a_1(Y_{E,NO,i} - Y_{B,NO,i}) \\ &\quad \text{(NO out)} \quad \text{(NO in)} \quad \text{(NO exchanged to bubble phase)} \\ &- a_{E,NO,i} Y_{E,NO,i} + R_{E,NO,c,i} \\ &\quad \text{(NO reduced by char)} \quad \text{(NO released during char combustion)} \\ &+ R_{E,NO,v,i} \quad (26) \\ &\quad \text{(NO released during volatiles combustion)} \end{aligned}$$

where

$$a_{E,NO,i} = a_m A_{T,i} \Delta Z_i (1 - \epsilon_{c,i} - \epsilon_{tube,i})$$

$$k_{E,NO,i} \frac{P}{R_g T_{E,i}} X_i, \text{ gmole/s}$$

## BUBBLE PHASE EQUATIONS

$$\begin{aligned} F_{BM,i} Y_{B,SO_2,i} &= F_{BM,i-1} Y_{B,SO_2,i-1} - a_1(Y_{B,SO_2,i} - Y_{E,SO_2,i}) \\ &\quad (\text{SO}_2 \text{ out}) \quad (\text{SO}_2 \text{ in}) \quad (\text{SO}_2 \text{ exchanged to emulsion phase}) \\ &\quad - \frac{a_{B,SO_2,i} Y_{B,SO_2,i}}{(\text{SO}_2 \text{ absorbed by limestone})} + \frac{R_{B,SO_2,c,i}}{(\text{SO}_2 \text{ released during char combustion})} \\ &\quad + \frac{R_{B,SO_2,v,i}}{(\text{SO}_2 \text{ released during volatiles combustion})} \end{aligned} \quad (27)$$

where

$$a_{B,SO_2,i} = A_{t,i} \Delta Z_i (\epsilon_{c,i} - \epsilon_{B,i}) (1 - \epsilon_{mf}) k_{rl} \left( \frac{P}{R_g T_i} \right), \text{ gmole/s}$$

$$\begin{aligned} F_{BM,i} Y_{B,NO,i} &= F_{BM,i-1} Y_{B,NO,i-1} - a_1(Y_{B,NO,i} - Y_{E,NO,i}) \\ &\quad (\text{NO out}) \quad (\text{NO in}) \quad (\text{NO exchanged to emulsion phase}) \\ &\quad - \frac{a_{B,NO,i} Y_{B,NO,i}}{(\text{NO reduced by char})} + \frac{R_{B,NO,c,i}}{(\text{NO released during char combustion})} \\ &\quad + \frac{R_{B,NO,v,i}}{(\text{NO released during volatiles combustion})} \end{aligned} \quad (28)$$

where

$$a_{B,NO,i} = a_m A_{t,i} \Delta Z_i (\epsilon_{c,i} - \epsilon_{\text{tube},i}) k_{B,NO,i} \frac{P}{R_g T_{B,i}} X_i, \text{ gmole/s}$$

## FREEBOARD EQUATIONS

$$\begin{aligned} F_{MT} Y_{SO_2,i} &= F_{MT} Y_{SO_2,i-1} + \frac{R_{SO_2,i}}{(\text{SO}_2 \text{ released})} - \frac{a_{SO_2,i} Y_{SO_2,i}}{(\text{SO}_2 \text{ absorbed by limestone})} \end{aligned}$$

where

$$a_{SO_2,i} = \left( \frac{P}{R_g T_i} \right) N_{A,i} \left( \frac{\pi d_{le,i}^3}{6} \right) k_{rl}, \text{ gmole/s} \quad (29)$$

$$\begin{aligned} F_{MT} Y_{NO,i} &= F_{MT} Y_{NO,i-1} + \frac{R_{NO,i}}{(\text{NO released})} - \frac{a_{NO,i} Y_{NO,i}}{(\text{NO reduced by char})} \end{aligned} \quad (30)$$

where

$$a_{NO,i} = \left( \frac{P}{R_g T_{B,i}} \right) N_{c,i} \pi d_{ce,i}^2 k_{NO,i}, \text{ gmole/s}$$

The boundary conditions are

$$Y_{E,SO_2,1} = Y_{B,SO_2,1} = Y_{E,NO,1} = Y_{B,NO,1} = 0.0$$

## SOLID PHASE MATERIAL BALANCE

The overall material balance for the solids in  $i^{\text{th}}$  compartment in terms of net solids flow  $W_{\text{net},i}$  is given by

$$\begin{aligned} W_{\text{net},i} &= W_{\text{net},i-1} + \frac{W_{fc,i} R_{ch}}{(\text{char feed})} + \frac{W_{fa,i}}{(\text{additives feed})} \\ &\quad - \frac{W_{D,i}}{(\text{solids withdrawal})} - r_i \quad (\text{char burnt}) \end{aligned} \quad (31)$$

The boundary condition is  $W_{\text{net},1} = 0.0$ .

The material balance for the carbon in  $i^{\text{th}}$  compartment is given as follows by introducing the backmix flow  $W_{\text{mix}}$ :

$$\begin{aligned} (W_{\text{mix},i} - W_{\text{net},i}) X_{i+1} &- [W_{\text{mix},i-1} - W_{\text{net},i-1} + W_{\text{mix},i} - W_{D,i}] X_i \\ &+ W_{\text{mix},i-1} = r_i - W_{fc,i} C_{ch} M_c \end{aligned} \quad (32)$$

where  $X_i$  is the weight fraction of carbon in the  $i^{\text{th}}$  compartment. The boundary conditions are

$$W_{\text{mix},1} = W_{\text{mix},M1} = 0.0$$

## ENERGY BALANCE

The energy balance for the  $i^{\text{th}}$  compartment is given as follows:

$$\begin{aligned} &C_S (W_{\text{mix},i} - W_{\text{net},i}) T_{i+1} \\ &\quad [\text{heat in from } (i+1)^{\text{th}} \text{ cell}] \\ &- C_S \{ (W_{\text{mix},i-1} - W_{\text{net},i-1} + W_{\text{mix},i} - W_{D,i}) + C_{gm} F_{MT} \} T_i \\ &\quad (\text{heat out from } i^{\text{th}} \text{ cell}) \\ &+ [C_S W_{\text{mix},i-1} + C_{gm} F_{MT}] T_{i-1} + r_i q_{ch} \\ &\quad [\text{heat in from } (i-1)^{\text{th}} \text{ cell}] \quad (\text{heat generated by char combustion}) \\ &+ \frac{g_{E,i} q_{v,CO}}{(\text{heat generated by volatiles combustion in emulsion phase})} + \frac{g_{B,i} q_v}{(\text{heat generated by volatiles combustion in bubble phase})} + \frac{g_{CO,i} q_{CO}}{(\text{heat generated by CO combustion})} \\ &- \frac{q_{cal} W_{fa,i}}{(\text{heat of calcination})} + (W_{fa,i} C_{sf} + W_{fc,i} C_{cf}) T_{sf,i} \\ &= A_{t,i} \Delta Z_i a_{HE,i} U_i (T_i - T_{w,i}) + A_{t,i} \Delta Z_i a_{HEW,i} U_{w,i} \\ &\quad (\text{heat removed by cooling tubes}) \quad (T_i - T_{\text{wall},i}) \quad (\text{heat losses through the walls}) \end{aligned} \quad (33)$$

## ENERGY BALANCE IN THE FREEBOARD

The following equations are obtained for energy balance in the freeboard in  $i^{\text{th}}$  compartment:

$$\begin{aligned} (W_{\text{ent},i} C_S + C_{gm} F_{MT}) T_{i-1} &+ r_i q_{ch} \\ &[\text{heat in from } (i-1)^{\text{th}} \text{ compartment}] \quad (\text{heat generated by char combustion}) \\ &+ \frac{g_{E,i} q_{v,CO}}{(\text{heat generated by volatiles combustion})} + \frac{g_{CO,i} q_{CO}}{(\text{heat generated by CO combustion})} \\ &- (W_{\text{ent},i} C_S + C_{gm} F_{MT}) T_i = A_{t,i} \Delta Z_i a_{HE,i} U_i (T_i - T_{w,i}) \\ &\quad (\text{heat out from } i^{\text{th}} \text{ cell}) \quad (\text{heat removed by cooling tubes}) \\ &\quad + A_{t,i} \Delta Z_i a_{HEW,i} U_{w,i} (T_i - T_{\text{wall},i}) \\ &\quad (\text{heat losses through the walls}) \end{aligned} \quad (34)$$

The correlations used in simulation of hydrodynamics of FBC are listed in Table 1. Table 2 indicates the assumed values for the parameters involved in the model. If, in the future, when additional data become available and improved correlations are developed, they can be easily substituted into the correlations used in the model. Algebraic equations obtained are solved using IBM's SSP routine, SIMQ.

## RESULTS AND DISCUSSION

The validity of the proposed fluidized bed combustor model is tested under a set of operating conditions based on the experimental data reported by the National Coal Board, England (1971), Gibbs and his associates in Sheffield (1975), the Exxon Research and Engineering Company, United States of America (1976) and NASA Lewis Research Center, Cleveland, Ohio (1978). Table 3 gives the dimensions of the various beds simulated and the configuration of heat exchange coils used.



TABLE 1. HYDRODYNAMICS CORRELATIONS USED IN THE MODEL

Equation No.	Variable	Correlation	Reference
1	Minimum fluidization velocity, $U_{mf}$ , cm/s	$U_{mf} = \left( \frac{\mu}{d_p \rho_g} \right) \left\{ \left[ 33.7^2 + \frac{0.0408 d_p^3 \rho_g (\rho_s - \rho_g) g}{\mu^2} \right]^{1/2} - 33.7 \right\}$	Wen and Yu (1966)
2	Bubble diameter, $D_B$ , cm	$D_B = D_{BM} - (D_{BM} - D_{B0}) \exp(-0.3z/D_I)$ $D_{BM} = 0.652 \{ A_t (U_0 - U_{mf}) \}^{0.4}$ $D_{B0} = 0.347 \{ A_t (U_0 - U_{mf}) / nd \}^{0.4}$	Mori and Wen (1975)
3	Bubble velocity, $U_B$ , cm/s	$U_B = U_0 - U_{mf} + 0.711 \sqrt{g D_B}$	Davidson and Harrison (1963)
4	Bubble fraction, $\epsilon_B$	$\epsilon_B = (U_0 - U_{mf}) / U_B$	Kunii and Levenspiel (1968)
5	Cloud fraction, $\epsilon_c$	$\epsilon_c = \epsilon_B \alpha_b / (\alpha_b - 1)$ , $\alpha_b = \frac{\epsilon_{mf} U_B}{U_{mf}}$	Kunii and Levenspiel (1968)
6	Gas interchange coefficient, $K_{BE}$ , 1/s	$K_{BE} = 11/D_B$	Kobayashi et al. (1967)
7	Solids mixing rate, $W_{mix}$ , g/s	$W_{mix} = (U_0 - U_{mf}) A_t f_w (1 - \epsilon_{mf}) \rho_s$	Rajan et al. (1978)
8	Attrition rate, $R_a$ , g/s	$R_a = K(U_0 - U_{mf}) M_b$ $K = 9.11 \times 10^{-8} \sim 2.73 \times 10^{-8}$ 1/cm	Merrick and Highley (1974)

TABLE 2. PARAMETERS IN THE MODEL

Bed to tube head transfer coefficient,  $U = 0.03203$ , J/s cm<sup>2</sup> °K  
 Freeboard heat transfer coefficient =  $(1/3)U$ , J/s cm<sup>2</sup> °K  
 Bed to wall heat transfer coefficient =  $0.00879$ , J/s cm<sup>2</sup> °K  
 Solids mixing parameter,  $f_w = 0.075 \sim 0.3$   
 Fraction of wake solids thrown into the freeboard,  $f_{sw} = 0.1 \sim 0.5$   
 Cooling water temperature =  $300^\circ\text{K}$   
 Wall heat transfer coefficient in the freeboard =  $0.001047$  J/s cm<sup>2</sup> °K  
 Heat capacity of solids,  $C_s = 0.9001$  J/g °K  
 Heat capacity of gas,  $C_{gm} = 28.47 + 2.0934 \times 10^{-3} t(^{\circ}\text{C})$   
 Density of limestone =  $2.4$  g/cm<sup>3</sup>  
 Density of coal =  $1.4$  g/cm<sup>3</sup>

Figure 3 shows an example of simulation based on the experiment performed by National Coal Board. The size distributions of the particles in the bed and in the elutriated material for a given feed size distribution calculated from the model are compared with the experimental data under the set of operating conditions specified in the figure. The solid lines in Figure 3 representing the results of the model simulation indicate close agreement with experimental data. The fine particles in the feed are quickly entrained by the gas stream, and hence the bed particles size is larger than that of the feed particles. The fine particles are splashed into the freeboard by the bursting bubbles at the bed surface. Bigger particles fall back to the bed, while the smaller ones are completely elutriated.

If the heat exchange coils are closely packed in the bed, the free moving, coalescing bubbles are constrained and may be broken as they impinge on the walls of the tubes. Hence, in such a bed the solids movement is retarded, which in turn affects the temperature profile. In the model, the solids mixing in the bed is represented by the mixing coefficient  $f_w$ . For poor solids mixing,  $f_w$  takes on low values (0.05 to 0.2), and for vigorous mixing it takes high values (0.2 to 0.4). A simulation of the operation of NASA fluid bed combustor is presented in Figure 4. In this combustor, closely packed horizontal tubes are employed for heat removal, and, hence, the solids mixing is poor which is clearly shown by the nonuniform temperature profile and the nonuniform carbon concentration profile in the bed. Carbon concentration peaks at the coal feed point and decreases rapidly within the bed as combustion proceeds. Because of the higher concentration of carbon and oxygen near the coal feed point near the distributor, the combustion rate and the heat release rate are higher than the remaining part of the bed. This results in a high temperature zone near the coal feed point. On the other hand, in the freeboard region, though combustion takes place owing to the heat losses through the wall, the temperature drops.

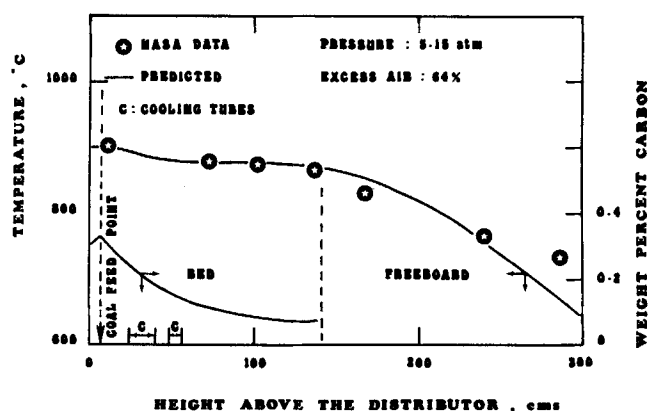


Figure 4. Temperature and carbon concentration profiles in the bed.

Figure 5 shows the effect of fluidizing velocity on sulfur retention efficiency. At low velocities, elutriation is small, and hence the average bed particle size is small. This implies a greater reactivity of the limestone particles. Also, the gas and solids residence times are increased. Hence, a higher sulfur dioxide retention efficiency is obtained. But, at higher fluidizing velocities, entrainment is large, and the particles entrained are also larger. Bed particle sizes are consequently larger, resulting in lower reactivities. At higher superficial velocities, residence time is also short. A combination of these effects results in a lower sulfur dioxide retention efficiency. Figure 6 shows the

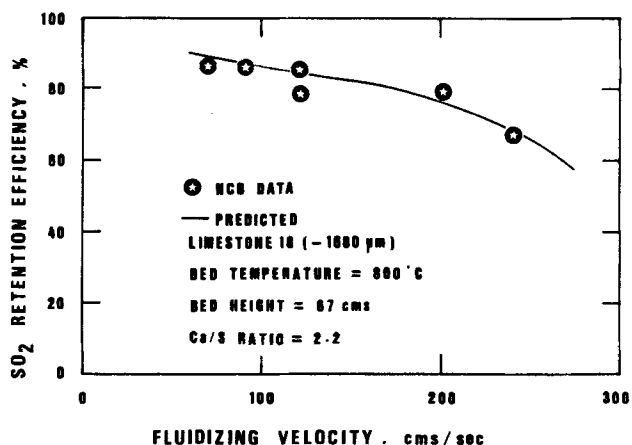


Figure 5. Effect of fluidizing velocity in sulfur dioxide retention.

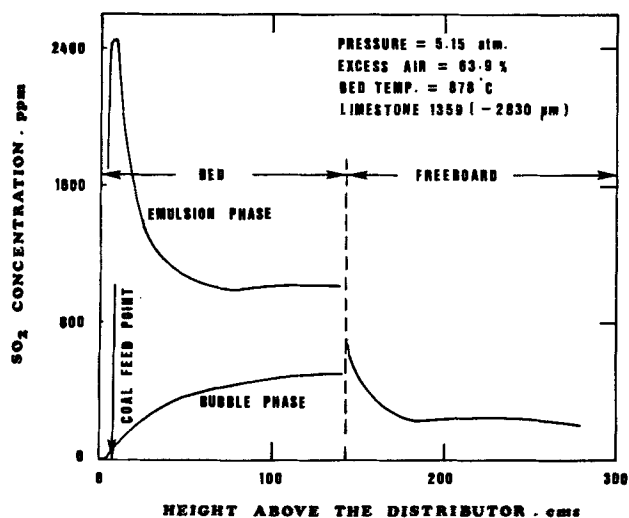


Figure 6. Sulfur dioxide concentration profile in the combustor.

sulfur dioxide concentration profiles obtained from the simulation of a NASA combustor. Near the coal feed point, because of the combustion of volatiles, a large proportion of sulfur dioxide is released into the emulsion phase. A high concentration of sulfur dioxide is seen at this location. Sulfur dioxide is then absorbed by the calcined limestone particles in the bed, and its concentration in the emulsion phase decreases as a function of height above the distributor. The gases leaving the bed surface come in contact with the fine limestone particles entrained into the freeboard, and sulfur capture is appreciable in the freeboard region. Also, in the case of a NASA combustor, since the cross-sectional area of the freeboard region increases as a function of bed height, the gas and solids residence time in the freeboard increases. Hence, the sulfur dioxide retention is high, and its concentration in the freeboard is low.

The effect of bed temperature on nitric oxide emission is shown in Figure 7. The average carbon concentration in the bed which is closely related to nitric oxide reduction is also shown in the figure. Nitric oxide concentration at the exit in the flue gas increases with the bed temperature, while the average carbon concentration in the bed decreases. At low temperatures, nitric oxide formed is reduced by the larger amount of char in the bed. At higher temperatures, the nitric oxide emission increases, since the char content is low, affecting the nitric oxide-char reaction rate. At temperatures above 825°C, the nitric oxide emission plateaus off. This is due to the fact that while the nitric oxide reduction rate by char above this temperature becomes fast, the char content in the bed is significantly lowered.

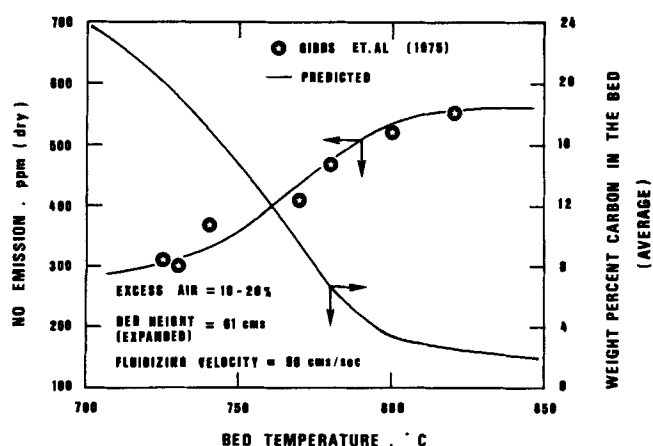


Figure 7. Effect of temperature on nitric oxide emission.

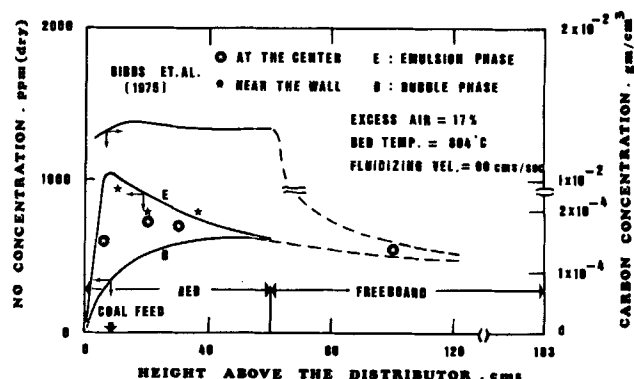


Figure 8. Nitric oxide and carbon concentration profiles in the bed.

Figure 8 is an example of the nitric oxide concentration profiles in the bubble and emulsion phases. Data points are the time averaged nitric oxide concentrations obtained experimentally (Gibbs et al., 1975) near the wall and at the center of the bed. The nitric oxide concentration near the wall is higher than that at the center of the bed. The probability of a probe sampling the bubble is higher at the center than near the wall, since the proportion of the bubbles is small near the walls. These results indicate that nitric oxide is preferentially formed in the emulsion phase owing to the release and subsequent combustion of volatiles in the emulsion phase. Higher concentrations of nitric oxide in the emulsion phase near the coal feed point are the results of rapid evolution and combustion of volatiles from coal in this region. The nitric oxide concentration in the bubble phase increases because of char and volatiles combustion. Fig-

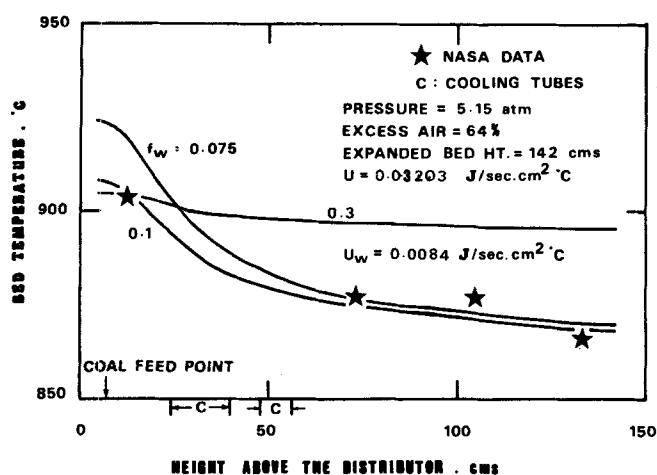


Figure 9. Effect of solids mixing on the bed temperature profile.

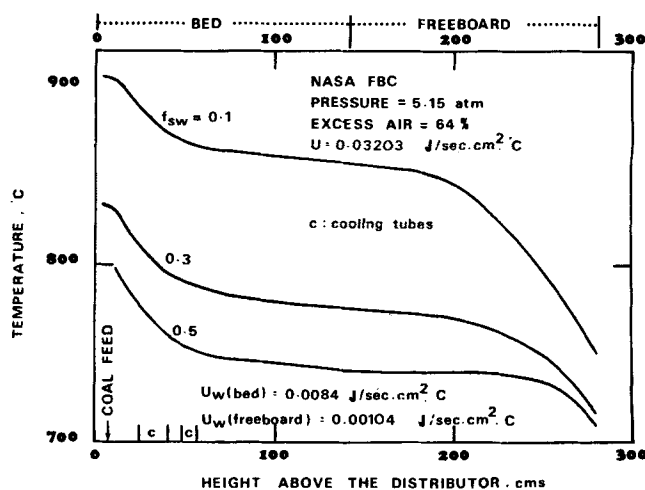
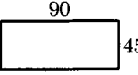
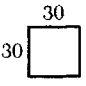

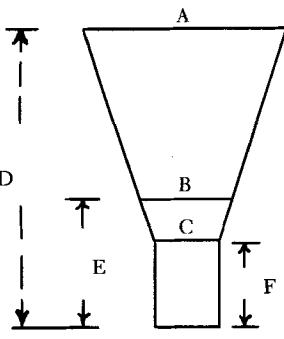


Figure 10. Effect of solids entrainment on the temperature profile.

TABLE 3. DIMENSIONS OF FBC EXAMINED

Type	Bed cross section, cm	Specific surface area, $\text{cm}^2/\text{cm}^3$ bed	Tube outside diameter, cm	Vertical pitch, cm	Horizontal pitch, cm	Tube configuration
NCB		0.15	5.4	9.9	11.4	Horizontal staggered
Gibbs et al. (1975)		—	1.25	—	—	—
Exxon mini plant		0.205	1.9	—	5.5	Horizontal serpentine
		0.149	1.9	—	—	Vertical coils
NASA		0.1744	1.25	8.0	2.86	Horizontal In line

$A = 52.8$     $E = 81.3$   
 $B = 29.2$     $F = 62.7$   
 $C = 22.7$   
 $D = 280$

ure 8 also indicates the nitric oxide concentrations in the freeboard. In the freeboard, both char combustion and nitric oxide reduction takes place. When the char burns, nitric oxide is released from the nitrogen contained in the char. These two competing reactions determine the total nitric oxide emission at the outlet of the combustor.

Two of the important parameters in the model are the solids mixing parameter  $f_w$  and the fraction of wake solids thrown into the freeboard  $f_{sw}$ . The effects of these parameters on the temperature profile in the bed are shown in Figures 9 and 10. For this parametric study, the bed dimensions and cooling coils location are similar to the NASA fluid bed combustor (Table 3). In the future, when more accurate correlations are developed, these new correlations should be used for estimation of these parameters in the model. Figure 9 shows the effect of  $f_w$  on the

temperature profile in the bed. Low values of  $f_w$  represent poor solids mixing. When solids mixing is poor, most of the volatiles are released near the coal feed point. Combustion of these volatiles causes a rise in the temperature of the bed in the neighborhood of the solids feed point. As  $f_w$  increases, solids mixing becomes more vigorous, and heat liberated by the combustion of volatiles near the feed point is immediately dissipated by the rapidly mixing solids. Because of improved mixing, the bed temperature profile becomes uniform.

The extent of freeboard reactions depends on the solids hold up in the freeboard. Solids hold up in turn depends on the amount of solids thrown up into the freeboard by the bursting bubbles at the bed surface. The rate of entrainment of solids from the bed surface  $F_0$  is given by Equation (2) (Yates and Rowe, 1977). For a set of operating conditions, increasing the value of  $f_{sw}$  increases the solids splashing rate at the bed surface. If a large amount of solids is splashed, char elutriation from the combustor will also be large. This will result in lower combustion efficiency and hence a lower temperature in the bed. The

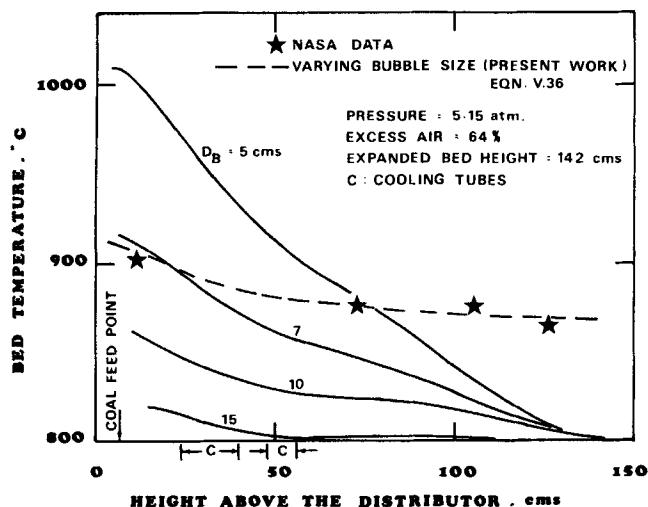


Figure 11. Effect of bubble size (or compartment size) on the bed temperature profile.

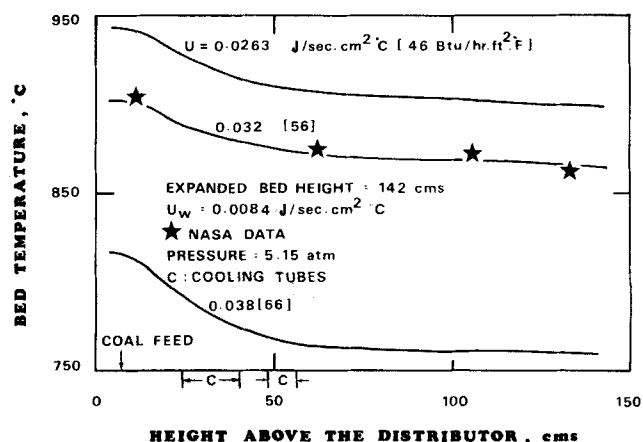


Figure 12. Effect of bed to tube heat transfer coefficient on the bed temperature.

temperature drop in the freeboard decreases as  $f_{sw}$  increases because of increased combustion in the freeboard. This is clearly illustrated in Figure 10. It should be borne in mind that the NASA fluidized bed combustor is a small unit, and heat losses from the wall in the freeboard are considerable. If the bed is bigger in size than the one used here, the heat losses through the walls will be minimal. Also, with good insulation, heat losses can be reduced. In large commercial combustors, if the entrainment is increased, combustion of char in the freeboard will also increase, resulting in higher temperatures in the freeboard. Hence it is seen that the parameter  $f_{sw}$  is critical and has to be carefully evaluated in order to properly account for the freeboard reactions.

Figure 11 brings out the effect of bubble size (or the compartment size, since compartment size is taken as the same as bubble size) on the bed temperature profile. When a single bubble diameter is used as an adjustable parameter, a small value for the bubble diameter tends to overestimate the combustion rate in the bed. This is because of increased mass transfer of oxygen to the emulsion phase from the bubble phase. This results in steep temperature profiles. As the bubble diameter is increased, the profile becomes less steep, and also the average temperature decreases because of less combustion in the bed. Figure 11 also compares the present work with the experimental data. Clearly, it is seen that bubble size cannot be assumed as an arbitrary parameter, and the coalescence of bubbles has to be incorporated in any realistic FBC model.

Figure 12 is a parametric study of the effect of bed to tube heat transfer coefficient on the temperature profile in the bed. Changes in the value of the heat transfer coefficient do not significantly affect the shape of the temperature profile but affect the level of bed temperature. As can be seen from Figure 12, if the actual heat transfer coefficient were  $0.03203 \text{ J/s cm}^2\text{C}$  ( $56 \text{ Btu/hr} \cdot \text{ft}^2 \cdot ^\circ\text{F}$ ), the assumption of a lower heat transfer coefficient of  $0.02637 \text{ J/s} \cdot \text{cm}^2\text{C}$  ( $46 \text{ Btu/hr} \cdot \text{ft}^2 \cdot ^\circ\text{F}$ ) would result in a temperature difference of about  $40^\circ\text{C}$  above the actual temperature. So it is apparent that an accurate estimation of the heat transfer coefficient for a wide range of design is critical to make accurate predictions of bed temperatures.

## ACKNOWLEDGMENT

This work was supported by a grant from NASA Lewis Research Center, Cleveland, Ohio, and the energy research funds from the State of West Virginia. The assistance of Mr. P. R. Rao in proofing of the paper is appreciated.

## NOTATION

$A_t$	= cross-sectional area of the bed, $\text{cm}^2$
$a_{HE}$	= specific heat transfer area of the tubes, $\text{cm}^2/\text{cm}^3 \text{ FBC volume}$
$a_{HEW}$	= specific heat transfer area of the walls, $\text{cm}^2/\text{cm}^3 \text{ FBC volume}$
$a_x$	= proportion of total abrasion fines in the $x^{\text{th}}$ size fraction
$b_x$	= weight fraction of bed material in the $x^{\text{th}}$ size fraction
$C_{cf}$	= heat capacity of coal feed, $\text{J/g } ^\circ\text{C}$
$C_{\text{CO}_2}$	= concentration of carbon dioxide, $\text{gmole}/\text{cm}^3$
$C_{ch}$	= carbon content in char, $\text{g carbon/g char}$
$C_{gm}$	= molar heat capacity of gas, $\text{J/gmole } ^\circ\text{C}$
$C_{\text{NO}}$	= concentration of nitric oxide, $\text{gmole}/\text{cm}^3$
$C_s$	= heat capacity of solids, $\text{J/g } ^\circ\text{C}$
$C_{sf}$	= heat capacity of feed additives, $\text{J/g } ^\circ\text{C}$
$C_{\text{SO}_2}$	= concentration of sulfur dioxide, $\text{gmole}/\text{cm}^3$
$\text{CH}_4$	= wt. fraction methane in the volatiles
$\text{CO}$	= wt. fraction carbon monoxide in the volatiles
$D$	= molecular diffusivity for oxygen-nitrogen $\text{cm}^2/\text{s}$
$D_B$	= bubble diameter, $\text{cm}$
$D_{B0}$	= bubble diameter at the distributor level, $\text{cm}$
$D_{BM}$	= fictitious maximum bubble diameter, $\text{cm}$
$D_t$	= diameter of FBC, $\text{cm}$
$d_c$	= diameter of char particle in the bed, $\text{cm}$

$d_{ce}$	= diameter of char particle entrained in the freeboard, $\text{cm}$
$d_l$	= diameter of limestone particle in the bed, $\text{cm}$
$d_{le}$	= diameter of limestone particle entrained in the freeboard, $\text{cm}$
$d_p$	= particle diameter, $\text{cm}$
$E_x$	= elutriation rate constant, $\text{g/s}$
$E_z$	= dispersion coefficient in the freeboard, $\text{cm}^2/\text{s}$
$F_{BM}$	= molar flow rate of gas in the bubble phase, $\text{gmole/s}$
$F_{EM}$	= molar flow rate of gas in the emulsion phase, $\text{gmole/s}$
$F_{MT}$	= total molar flow rate of gas in the combustor, $\text{gmole/s}$
$F_0$	= solids entrainment rate at the bed surface, $\text{g/s}$
$F_{0,x}$	= entrainment rate of particles of $x$ size fraction at bed surface
$f_{sw}$	= fraction of wake solids thrown into the freeboard
$f_w$	= solids mixing parameter, ratio of wake volume to the bubble volume including the wakes
$G$	= gas flow rate, $\text{g/s}$
$g$	= acceleration due to gravity, $\text{cm/s}^2$
$g_B$	= volatiles burning rate in the bubble phase, $\text{gmole/s}$
$g_{\text{CO}}$	= carbon monoxide burning rate, $\text{gmole/s}$
$g_E$	= volatiles burning rate in the emulsion phase, $\text{gmole/s}$
$\text{H}_2$	= wt. fraction hydrogen in the volatiles
$\text{H}_2\text{O}$	= wt. fraction water in the volatiles
$h$	= height above the bed surface, $\text{cm}$
$K$	= attrition rate constant, $1/\text{cm}$
$K_{BE}$	= gas exchange coefficient, $1/\text{s}$
$k_{B,\text{NO}}$	= nitric oxide reduction rate constant in the bubble phase, $\text{cm/s}$
$k_{\text{CO}_2}$	= carbon-carbon dioxide chemical reaction rate constant, $\text{cm/s}$
$k_{E,\text{NO}}$	= nitric oxide reduction rate constant in the emulsion phase, $\text{cm/s}$
$k_{\text{NO}}$	= nitric oxide reduction rate constant, $\text{cm/s}$
$k_c$	= overall rate constant for char combustion, $\text{cm/s}$
$k_{c,B}$	= overall rate constant for char combustion in bubble phase, $\text{cm/s}$
$k_{c,E}$	= overall rate constant for char combustion in emulsion phase, $\text{cm/s}$
$k_{cf}$	= gas film diffusion rate constant, $\text{g}/\text{cm}^2 \cdot \text{s} \cdot \text{atm}$
$k_{cR}$	= chemical reaction rate constant for char combustion, $\text{g}/\text{cm}^2 \cdot \text{s} \cdot \text{atm}$
$k_{rl}$	= overall volume reaction rate constant for limestone-sulfur dioxide reaction, $1/\text{s}$
$k_x$	= abrasion rate constant for the $x^{\text{th}}$ size fraction, $1/\text{s}$
$k'_{rl}$	= chemical reaction rate constant for limestone-sulfur dioxide reaction, $1/\text{s}$
$M$	= weight of particles remaining in the bed after the size reduction from the original size to $d_x$
$M_b$	= weight of bed material, $\text{g}$
$M_c$	= atomic weight of carbon, $\text{g/g atom}$
$M_x$	= weight of bed material in the $x^{\text{th}}$ size fraction
$N_A$	= number of limestone particles in the $i^{\text{th}}$ compartment in the freeboard
$N_c$	= number of char particles in the $i^{\text{th}}$ compartment in the freeboard
$N_{Pe}$	= Peclet number
$N_{Re}$	= Reynolds number
$N_{Sc}$	= Schmidt number
$n_d$	= number of orifices in the distributor
$P$	= average pressure of the FBC, $\text{atm}$
$P_{\text{O}_2}$	= partial pressure of oxygen, $\text{atm}$
$P_1$	= proportion of fines recycles to the bed from the primary cyclone
$P_2$	= proportion of fines recycled to the bed from the secondary cyclone
$q_{cal}$	= heat of calcination of limestone, $\text{J/g}$
$q_{ch}$	= heat of combustion of char, $\text{J/g}$
$q_v$	= heat of combustion of volatiles (complete burning), $\text{J/gmole}$
$q_{v,\text{CO}}$	= heat of combustion of volatiles (partial burning), $\text{J/gmole}$

$q_{1x}$  = collection efficiency of the primary cyclones for the  $x^{\text{th}}$  size fraction  
 $q_{2x}$  = collection efficiency of the secondary cyclones for the  $x^{\text{th}}$  size fraction  
 $R$  = gas constant, 8 319.17, J/kg-mole °K  
 $R_a$  = attrition rate, g/s  
 $R_{B,NO,c}$  = nitric oxide release rate in the bubble phase due to char combustion, gmole/s  
 $R_{B,NO,v}$  = nitric oxide release rate in the bubble phase due to volatiles combustion, gmole/s  
 $R_{B,SO_2,c}$  = sulfur dioxide release rate in the bubble phase due to char combustion, gmole/s  
 $R_{B,SO_2,v}$  = sulfur dioxide release rate in the bubble phase due to volatiles combustion, gmole/s  
 $R_{ch}$  = char produced per unit g of coal fed, g/g  
 $R_{CO}$  = carbon monoxide released during devolatilization, gmole/s  
 $R_{CO_2}$  = carbon dioxide released during devolatilization, gmole/s  
 $R_{E,NO,c}$  = nitric oxide release rate in the emulsion phase due to char combustion, gmole/s  
 $R_{E,NO,v}$  = nitric oxide release rate in the emulsion phase due to volatiles combustion, gmole/s  
 $R_{E,SO_2,v}$  = sulfur dioxide release rate in the emulsion phase due to volatiles combustion, gmole/s  
 $R_g$  = gas constant, 82.06 atm · cm<sup>3</sup>/gmole °K  
 $R_{NO}$  = nitric oxide release rate, gmole/s  
 $R_{SO_2}$  = sulfur dioxide release rate, gmole/s  
 $R_v$  = volatiles released, gmole/s  
 $R_x$  = elutriation rate of close size fraction  $x$  for given operating conditions  
 $r_{CO}$  = rate of combustion of carbon monoxide, gmole/cm<sup>3</sup> s  
 $r_i$  = char combustion rate in  $i^{\text{th}}$  compartment, g/s  
 $r_c^*$  = char combustion rate, gmole/s · particle  
 $S_g$  = effective specific surface area of limestone, cm<sup>2</sup>/g  
 $T$  = temperature in the bed, °K  
 $T_B$  = mean temperature in the boundary layer of the char particle in the bubble phase, °K; also in the freeboard, °K  
TDH = transport disengaging height, cm  
 $T_c$  = char particle temperature °K  
 $T_E$  = mean temperature in the boundary layer of the char particle in the emulsion phase, °K  
 $T_m$  = mean temperature in the boundary layer of the char particle, °K  
 $T_{sf}$  = solids feed temperature, °K  
 $T_w$  = cooling water temperature, °K  
 $T_{wall}$  = average FBC wall temperature, °K  
 $t$  = temperature, °C  
 $t_b$  = burning time of a char particle, s  
Tar = wt. fraction tar in the volatiles  
 $U$  = bed to tube hat transfer coefficient, J/s · cm<sup>2</sup> °C  
 $U_B$  = bubble velocity, cm/s  
 $U_{mf}$  = minimum fluidization velocity, cm/s  
 $U_0$  = superficial gas velocity or fluidization velocity, cm/s  
 $\bar{U}_t$  = terminal velocity of the particle, cm/s  
 $U_w$  = bed to wall heat transfer coefficient, J/s · cm<sup>2</sup> °C  
 $V$  = volatiles yield during devolatilization, % of coal daf  
 $V_{CO}$  = carbon monoxide produced due to volatiles burning, gmole CO/gmole volatile  
 $V_{CO_2}$  = carbon dioxide produced due to volatiles burning, gmole CO<sub>2</sub>/gmole volatile  
 $V_N$  = volatile nitrogen in coal, g/g, dry basis (d.b.)  
 $V_S$  = volatile sulfur in coal, g/g, dry basis (d.b.)  
VM = proximate volatile matter in the coal, % of coal daf  
 $W_D$  = solids withdrawal rate, g/s  
 $W_{ent}$  = solids entrainment rate, g/s  
 $W_{f,a}$  = additives feed rate, g/s  
 $W_{f,c}$  = coal feed rate, g/s  
 $W_{f,x}$  = solids feed rate of  $x^{\text{th}}$  size fraction, g/s  
 $W_{mix}$  = solids mixing rate, g/s  
 $W_{net}$  = net flow rate of solids, g/s

$W_x$  = rate of transfer of particles from size fraction  $x$  to fraction  $x + 1$  by size reduction, g/s  
 $X$  = weight fraction carbon in the bed  
 $X_{O_2}$  = oxygen required for partial combustion of volatiles, gmole O<sub>2</sub>/gmole volatile  
 $X_{O_2,c}$  = oxygen required for complete combustion of volatiles, gmole O<sub>2</sub>/mole volatile  
 $X_{VM}$  = proximate volatile matter content of coal, g/g coal (daf)  
 $Y_B$  = mole fraction oxygen in the bubble phase  
 $Y_{B,CO_2}$  = mole fraction carbon dioxide in the bubble phase  
 $Y_{B,NO}$  = mole fraction nitric oxide in the bubble phase  
 $Y_{B,SO_2}$  = mole fraction sulfur dioxide in the bubble phase  
 $Y_{CO}$  = mole fraction carbon monoxide  
 $Y_{CO_2}$  = mole fraction carbon dioxide  
 $Y_E$  = mole fraction oxygen in the emulsion phase  
 $Y_{E,CO}$  = mole fraction carbon monoxide in the emulsion phase  
 $Y_{E,CO_2}$  = mole fraction carbon dioxide in the emulsion phase  
 $Y_{E,NO}$  = mole fraction nitric oxide in the emulsion phase  
 $Y_{E,SO_2}$  = mole fraction sulfur dioxide in the emulsion phase  
 $Y_{E,v}$  = mole fraction volatiles in the emulsion phase  
 $Y_{H_2O}$  = mole fraction water  
 $Y_O$  = mole fraction oxygen  
 $Y_{NO}$  = mole fraction nitric oxide  
 $Y_{SO_2}$  = mole fraction sulfur dioxide  
 $Y_v$  = mole fraction volatiles  
 $Z$  = height above the distributor, cm;  $\Delta Z$  compartment size, cm

#### Greek Letters

$\epsilon_B$  = bubble fraction  
 $\epsilon_c$  = cloud fraction including bubble  
 $\epsilon_{mf}$  = void fraction at minimum fluidization  
 $\epsilon_{tube}$  = volume fraction of tubes  
 $\lambda_l$  = reactivity of limestone  
 $\mu$  = viscosity of gas, g/cm · s  
 $\rho_{c,ch}$  = density of carbon in char, g/cm<sup>3</sup>  
 $\rho_{ch}$  = density of char, g/cm<sup>3</sup>  
 $\rho_g$  = density of gas, g/cm<sup>3</sup>  
 $\rho_s$  = density of solids  
 $\phi$  = mechanism factor of char combustion  
 $\phi_B$  = mechanism factor in the freeboard  
 $\phi_E$  = mechanism factor in the emulsion phase

#### Subscripts

$x$  =  $x^{\text{th}}$  size fraction  
 $i$  =  $i^{\text{th}}$  compartment

#### LITERATURE CITED

- Amitin, A. V., I. G. Martyushin and D. A. Gurevich, "Dusting in the Space Above the Bed in Converters with a Fluidized Catalyst Bed," *Chem. Technol. Fuels Oils*, 3-4, 181 (1968).  
Arthur, J. R., "Reactions Between Carbon and Oxygen," *Trans. Faraday Soc.*, 47, 164 (1951).  
Avedesian, M. M., and J. F. Davidson, "Combustion of Carbon Particles in a Fluidized Bed," *Trans. Inst. Chem. Engrs.*, 51, 121 (1973).  
Baron, R. E., J. L. Hodges and A. F. Sarofim, "Mathematical Model for Predicting Efficiency of Fluidized Bed Steam Generators," paper presented at AIChE 70th Annual Meeting, New York (Nov., 1977).  
Becker, H. A., J. M. Beer and B. M. Gibbs, "A Model for the Fluidized Bed Combustor of Coal," *Inst. Fuel Symp. Series*, Paper A1 (1975).  
Beer, J. M., "The Fluidized Combustion of Coal," paper presented at 16th International Symposium on Combustion, The Combustion Institute, 439-460 (1977).  
Borghi, G., A. F. Sarofim and J. M. Beer, "A Model of Coal Devolatilization and Combustion in Fluidized Beds," paper presented at AIChE 70th Annual Meeting, New York (Nov., 1977).  
Borgwardt, R. H., "Kinetics of the Reaction of SO<sub>2</sub> with Calcined Limestone," *Environ. Sci. Tech.*, 4, 59 (1970).  
Campbell, E. K., and J. F. Davidson, "The Combustion of Coal in Fluidized Beds," *Inst. Fuel Symp. Series*, Paper A2 (1975).

- Caram, H. S., and N. R. Amundson, "Diffusion and Reaction in a Stagnant Boundary Layer About a Carbon Particle," *Ind. Eng. Chem. Fundamentals*, **16**, 171 (1977).
- Chen, T. P., and S. C. Saxena, "A Mechanistic Model Applicable to Coal Combustion in Fluidized Beds," *AIChE Symposium Ser. No. 176*, **74**, 149 (1978).
- Davidson, J. F., and D. Harrison, *Fluidized Particles*, Cambridge Univ. Press (1963).
- Exxon Research and Engineering Company, "Studies of the Pressurized Fluidized Bed Coal Combustion Process," EPA-600/7-76-011, Linden, N.J. (1976).
- Field, M. A., D. W. Gill, B. B. Morgan and P. G. W. Hawksley, "Combustion of Pulverized Coal," BCURA (1967).
- Fine, D. H., S. M. Slater, A. F. Sarofim and G. C. Williams, "Nitrogen in Coal as a Source of Nitrogen Oxide Emission from Furnaces," *Fuel*, **53**, 120 (1974).
- Fournol, A. B., M. A. Bergougnou and C. G. J. Baker, "Dilute Phase Hold-Up in a Large Gas Fluidized Bed," *Can. J. Chem. Eng.*, **51**, 401 (1973).
- Gibbs, B. M., F. J. Pereira and J. M. Beer, "Coal Combustion and NO Formation in an Experimental Fluidized Bed," *Inst. Fuel Symp. Series*, Paper D6 (1975).
- Gibbs, B. M., "A Mechanistic Model for Predicting the Performance of a Fluidized Bed Coal Combustor," *ibid.*, Paper A5 (1975).
- Gordon, A. L., and N. R. Amundson, "Modeling of Fluidized Bed Reactors—IV: Combustion of Carbon Particles," *Chem. Eng. Sci.*, **31**, 1163 (1976).
- Gregory, D. R., and R. F. Littlejohn, "A Survey of Numerical Data on the Thermal Decomposition of Coal," *The BCURA Monthly Bulletin*, **29**, No. 6, 173 (1965).
- Horio, M., S. Mori and I. Muchi, "A Model Study for the Development of Low  $\text{NO}_x$  Fluidized Bed Combustors," Proc. of 5th FBC Conference, Washington, D.C. (1977).
- Horio, M., and C. Y. Wen, "Analysis of Fluidized Bed Combustion of Coal With Limestone Injection," Proc. of Int. Fluidization Conference, Pacific Grove, Calif. (1975).
- , "Simulation of Fluidized Bed Combustors: Part I Combustion Efficiency and Temperature Profile," *AIChE Symposium Ser. No. 176*, **74**, 101 (1978).
- Hottel, H. C., G. C. Williams, N. M. Nerheim and G. R. Schneider, "Burning Rate of Carbon Monoxide," 10th International Symposium on Combustion, 111 (1965).
- Ishida, M., and C. Y. Wen, "Effect of Solid Mixing on Non-Catalytic Solid-Gas Reactions in a Fluidized Bed," *AIChE Symposium Ser.*, **No. 128**, **69**, 1 (1973).
- Loison, R., and R. Chuvwin, "Pyrolyse Rapide du Charbon," *Chimie et Industrie*, **91**, 269 (1964).
- Merrick, D., and J. Highley, "Particle Size Reduction and Elutriation in a Fluidized Bed Process," *AIChE Symposium Ser. No. 137*, **70**, 366 (1974).
- Mori, S., and C. Y. Wen, "Estimation of Bubble Diameter in Gaseous Fluidized Beds," *AIChE J.*, **21**, 109 (1975).
- NASA Lewis Research Center, Cleveland, Ohio, Private Communication (1978).
- National Coal Board, "Reduction of Atmospheric Pollution," EPA-PB-210-673, London, England (1971).
- Nazemi, A., M. A. Bergougnou and C. G. J. Baker, "Dilute Phase Hold-Up in a Large Gas Fluidized Bed," *AIChE Symposium Ser. No. 141*, **70**, 98 (1974).
- Oguma, A., N. Yamada, T. Furusawa and D. Kunii, "Reduction Reaction Rate of Char With  $\text{NO}$ ," Preprint for 11th Fall Meeting of Soc. of Chem. Eng., Japan, 121 (1971).
- Park, D., O. Levenspiel and T. J. Fitzgerald, "A Model for Large Scale Atmospheric Fluidized Bed Combustors," paper presented at 72nd Annual AIChE Meeting, San Francisco, Calif. (Nov., 1979).
- Pereira, F. J., and J. M. Beer, "A Mathematical Model of NO Formation and Destruction in Fluidized Combustion of Coal," *Fluidization*, Proc. of Second Eng. Foundation Conf., Trinity College, Cambridge, England (1978).
- Rajan, R., R. Krishnan and C. Y. Wen, "Simulation of Fluidized Bed Combustion: Part II: Coal Devolatilization and Sulphur Oxides Retention," *AIChE Symposium Ser. No. 176*, **74**, 112 (1978).
- Sarofim, A. F., and J. M. Beer, "Modeling of Fluidized Bed Combustion," *Colloquium on Coal Combustion*, 189 (1979).
- Wen, C. Y., and L. H. Chen, "A Model for Coal Pyrolysis," Division of Fuel Chemistry, ACS, Preprint, **24**, 141 (1979).
- Wen, C. Y., and L. T. Fan, *Model for Flow Systems and Chemical Reactors*, Dekker, New York (1975).
- Wen, C. Y., and M. Ishida, "Reaction Rate of Sulphur Dioxide With Particles Containing Calcium Oxide," *Environ. Sci. Tech.*, **1**, 103 (1973).
- Wen, C. Y., and Y. H. Yu, "A Generalized Method for Predicting the Minimum Fluidization Velocity," *AIChE J.*, **12**, 610 (1966).
- Yates, J. G., and P. N. Rowe, "A Model for Chemical Reaction in the Freeboard Region Above a Fluidized Bed," *Trans. Inst. Chem. Engrs.*, **55**, 137 (1977).
- Zenz, F. A., and N. A. Weil, "A Theoretical-Empirical Approach to the Mechanism of Particle Entrainment from Fluidized Beds," *AIChE J.*, **4**, 472 (1958).

Manuscript received May 14, 1979; revision received January 17, and accepted January 23, 1980.

# Nucleation and Evolution of Slag Droplets in Coal Combustion

KWAN H. IM

and

PAUL M. CHUNG

Argonne National Laboratory  
Argonne, Illinois

Kinetics governing the nucleation and size variation of the slag droplets are first analyzed. Governing conservation equations are then formulated for the droplets and the surrounding gas-vapor mixture. These equations are solved numerically for the environments representing a typical flow through the channel and diffuser of a coal fired, MHD, power generation system. The average droplet size, total number density and the droplet size distribution are found to be rather strongly influenced by the total slag mass fraction and the supersaturation ratio.

## SCOPE

One of the added complexities associated with the flow of the coal generated plasma, through the MHD channel and the after gas system, is caused by the residual slag invariably carried over to the MHD channel from the coal combustor (see, for instance, Heywood and Womack, 1969; Way, 1974; Chung and Smith, 1977; Ubhayaker et al., 1976). The slag may be both in a liquid and vapor phase. In addition to physically

interacting with the electrode surfaces, the slag droplets, either carried into the channel or formed through nucleation, act as a strong electron sink (Martinez-Sanchez et al., 1977). Thus, the slag in the plasma could substantially affect the generator performance. Also, radiative heat transfer from the combustion gas to the surroundings is strongly influenced by the number density and size distribution of the droplets. In the subsequent after gas treatment system, condensation and removal of the slag must be accomplished among other gas cleaning and energy recovery processes. It is clear, therefore, that

Paul M. Chung is at the University of Illinois, Chicago Circle, Illinois.